

# THE COMPLEX ONE-SIDED INTEGRALS OF CAUCHY AND HADAMARD AND APPLICATION TO BOUNDARY ELEMENT METHOD

S. G. MOGILEVSKAYA\*

*Department of Mathematics, Kuzbass Technical University, Vesennia 28, Kemerovo 650026, Russia*

## SUMMARY

The definitions of complex integrals of Cauchy and Hadamard with the singular point coinciding with the end point of the integration curve are proposed. It is shown that the new integrals satisfy most of the properties of the regular ones, including the change of variables. It is also shown that the Cauchy principal value (CPV) and Hadamard finite-part (HFP) integrals can be considered as a sum of the new type integrals. The application to numerical solution by the boundary element method (BEM) and the complex hypersingular integral equation (CHSIE) for the multiregions of interacting elastic bodies and bodies with cracks and holes is discussed. The different ways to place the collocation points are considered. The numerical results for the problems of circular hole and circular elastic inclusion in infinite plate indicated that the appropriate choice of the approximating functions leads to a high accuracy of the calculation. Applications of the new technique to geomechanics problems are discussed. © 1998 John Wiley & Sons, Ltd.

Key words: boundary element method; complex hypersingular integrals

## 1. INTRODUCTION

In recent years the complex variable boundary element method (CVBEM) has been successfully used for the solution of plane harmonic (governed by Laplace's equation) and biharmonic (elasticity) problems.

The formulation of CVBEM was given at first for harmonic problems and may be found in References 1–5. The boundary integral equations (BIEs) in these works are obtained by using the Cauchy's integral theorem which expresses the value of some analytic inside domain function via its boundary values and taking the limit when the point approaches the boundary from the inside domain. The limit value is taken after the approximation of the unknown function and discretization of the boundary has been made.

The line and circular boundary elements and polynomial approximation of the unknown function are primarily used. The integrals of Cauchy's type are calculated in a closed form and the limit can be found easily even in the case when the point approaches the common point of the neighbouring elements.

Meanwhile, the BIEs for these problems can be obtained before the discretization of the boundary by using the concept of the CPV integral, Sokhotski–Plemelj's formulae or

\*Correspondence to: S. G. Mogilevskaya, Department of Mathematics, Kuzbass Technical University, Vesennia 28, Kemerovo 650026, Russia

holomorphy theorem. This way of obtaining BIEs have been extensively used for the solution of plane elasticity problems (see e.g. Reference 6 and 7 and references in it; also see References 8–14). It leads to complex singular BIEs (CSIEs). The theory of CSIEs is developed in detail and presented in the classical monograph by Muskhelishvili.<sup>7</sup> The CSIEs may then be solved numerically by a variety of numerical techniques (by BEM among them).

Recently, the theory of complex hypersingular integrals and CHSIEs has been created.<sup>15–19</sup> Some aspects of this theory were considered in References 20 and 21. The CHSIEs was shown to be a very effective tool to solve contact and crack problems.

But the problem arises when one solves the CSIE or CHSIE by BEM. As follows from the theory of complex CPV and HFP integrals, the point of singularity cannot be made to coincide with the end points of the integration curve (if the unknown function (or its derivative in the case of HFP integral) is not equal to zero at this point).

But according to the BEM technique the integrals over the whole boundary are represented by the sum of the integrals over each element. If the conventional collocation technique is used the collocation points may be chosen to coincide with the end points of the elements. In this case the integrals are not defined. To avoid this problem the collocation points are usually placed inside the elements.<sup>17,18</sup> The nodes of the Lagrange polynomials in this case may be chosen to coincide or not coincide with the end points.

Meanwhile, as we can see above, the CVBEM allows the situation of the collocation points at the end points of the elements. Moreover, in case of *real* variables the HFP integrals with the singular point at the end points of the integration interval were introduced by Hadamard<sup>22</sup> (so-called one-sided integrals of Hadamard). Kutt<sup>23</sup> suggested the numerical quadrature formulae for these integrals. It was also noticed in Reference 24 that the evaluation of the *real* CPV integrals by using the sum of the *real* one-sided HFP ones and the Kutt's quadrature rules may lead to more precious results. But real one-sided integral have a very unpleasant property. They are not independent of change of variables. It has been considered by some authors<sup>25,26</sup> as a main shortcoming of their employment.

The aim of the work presented here is to define the *complex one-sided* integrals of Cauchy and Hadamard and to apply the to the numerical treatment of CSIEs and CHSIEs by BEM. We show here that the introduction of new type of integrals does not lead to the ambiguity under the change of variables.

In the work presented, the new integrals are applied to the numerical solution of CHSIE for the multiregions of interacting elastic bodies and bodies with cracks, holes and inclusions.<sup>17</sup> This equation can be employed for the consideration of a number of important geomechanics problems. Different ways to place the collocation points are considered. The dependence of the results on the choice of the collocation points is investigated. The numerical results for the problems of circular hole and circular elastic inclusion in an infinite plate indicate that the appropriate choice of the approximating functions leads to a high accuracy of the calculation. The application of the new technique to geomechanical problems are discussed.

## 2. CAUCHY'S INTEGRAL WITH THE SINGULAR POINT AT THE END POINT OF THE INTEGRATION CURVE

Suppose, the boundary curve  $L$  is the open smooth arc  $ab$ . The generalization on the case of any piecewise smooth curve will be obvious from the following, mentioned below.

2.1. The integral  $I_a^1 = (1/2\pi i) \int_a^b \varphi(\tau) d\tau/(\tau - a)$

Enclose  $a$  with a circle of sufficiently small radius  $\varepsilon$  to cross  $ab$  at the point  $t_2$  (Figure 1). Suppose, the function  $\varphi(\tau)$  is a Holder continuous on  $ab$  (according to the terminology of Muskhelishvili<sup>7</sup> we will say that  $\varphi(\tau) \in H$  class on  $ab$ ).

Consider the *regular* integral

$$\frac{1}{2\pi i} \int_{t_2}^b \frac{\varphi(\tau) d\tau}{\tau - a} \quad (1)$$

It can be written as

$$\frac{1}{2\pi i} \int_{t_2}^b \frac{\varphi(\tau) d\tau}{\tau - a} = \frac{1}{2\pi i} \int_{t_2}^b \frac{\varphi(\tau) - \varphi(a)}{\tau - a} d\tau + \frac{\varphi(a)}{2\pi i} \ln \frac{b - a}{t_2 - a} \quad (2)$$

From the condition imposed on  $\varphi(\tau)$  it follows that

$$\lim_{\varepsilon \rightarrow 0} \frac{1}{2\pi i} \int_{t_2}^b \frac{\varphi(\tau) - \varphi(a)}{\tau - a} d\tau = \frac{1}{2\pi i} \int_a^b \frac{\varphi(\tau) - \varphi(a)}{\tau - a} d\tau \quad (3)$$

where the integral on the right-hand side of (3) is an improper one.

The second term in (2) is equal to

$$\frac{\varphi(a)}{2\pi i} \ln \frac{b - a}{t_2 - a} = \frac{\varphi(a)}{2\pi i} \ln \frac{b - a}{\exp(i\alpha_2)} - \frac{\varphi(a)}{2\pi i} \ln \varepsilon \quad (4)$$

where  $\alpha_2$  is the angle shown in Figure 1. When  $\varepsilon \rightarrow 0$  we have

$$\lim_{\varepsilon \rightarrow 0} \frac{\varphi(a)}{2\pi i} \ln \frac{b - a}{\exp(i\alpha_2)} = \frac{\varphi(a)}{2\pi i} \ln \frac{b - a}{\exp(i\alpha_a)} \quad (5)$$

where  $\alpha_a$  is the angle between the axis  $x$  and the tangent at the point  $a$  (the direction of the tangent is shown in Figure 1).

Suppose by definition

$$\frac{1}{2\pi i} \int_a^b \frac{\varphi(\tau) d\tau}{\tau - a} \stackrel{\text{def}}{=} \lim_{\varepsilon \rightarrow 0} \left[ \frac{1}{2\pi i} \int_{t_2}^b \frac{\varphi(\tau) d\tau}{\tau - a} + \frac{\varphi(a)}{2\pi i} \ln \varepsilon \right] \quad (6)$$

Taking into account (2)–(5), we get

$$\frac{1}{2\pi i} \int_a^b \frac{\varphi(\tau) d\tau}{\tau - a} = \frac{1}{2\pi i} \int_a^b \frac{\varphi(\tau) - \varphi(a)}{\tau - a} d\tau + \frac{\varphi(a)}{2\pi i} \ln \frac{b - a}{\exp(i\alpha_a)}. \quad (7)$$

The integral introduced by the formulae (6) and (7) will satisfy the following properties:

P.1. If  $\varphi_1(\tau), \varphi_2(\tau) \in H$  class on  $ab$ , then

$$\frac{1}{2\pi i} \int_a^b \frac{\varphi_1(\tau) + \varphi_2(\tau)}{\tau - a} d\tau = \frac{1}{2\pi i} \int_a^b \frac{\varphi_1(\tau) d\tau}{\tau - a} + \frac{1}{2\pi i} \int_a^b \frac{\varphi_2(\tau) d\tau}{\tau - a}$$

P.2. If  $k$  is any complex number, then

$$\frac{1}{2\pi i} \int_a^b k \frac{\varphi(\tau) d\tau}{\tau - a} = k \frac{1}{2\pi i} \int_a^b \frac{\varphi(\tau) d\tau}{\tau - a}$$

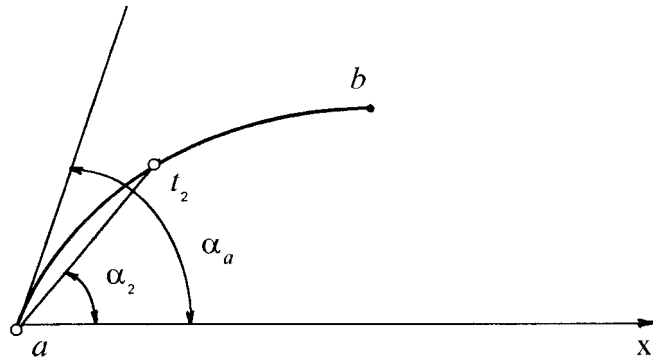


Figure 1. Geometry and co-ordinate system (singular point at the beginning of the arc)

P.3. If  $c \in ab$ , then

$$\frac{1}{2\pi i} \int_a^b \frac{\varphi(\tau) d\tau}{\tau - a} = \frac{1}{2\pi i} \int_a^c \frac{\varphi(\tau) d\tau}{\tau - a} + \frac{1}{2\pi i} \int_c^b \frac{\varphi(\tau) d\tau}{\tau - a}$$

P.4.

$$\frac{1}{2\pi i} \int_a^b \frac{\varphi(\tau) d\tau}{\tau - a} = \lim_{\varepsilon \rightarrow 0} \left[ \frac{1}{2\pi i} \int_a^b \frac{\varphi(\tau) d\tau}{\tau - t_2} + \frac{\varphi(a)}{2\pi i} \ln \varepsilon \right]$$

where the integral on the right-hand side is CPV one.

The properties P.1–P.3 may be proved quite easily by using formula (6).

To prove P.4 we rewrite the CPV integral in the form

$$\frac{1}{2\pi i} \int_a^b \frac{\varphi(\tau) d\tau}{\tau - t_2} = \frac{1}{2\pi i} \int_a^b \frac{\varphi(\tau) - \varphi(a)}{\tau - t_2} d\tau + \frac{\varphi(a)}{2\pi i} \int_a^b \frac{d\tau}{\tau - t_2}. \quad (8)$$

The difference  $\varphi(\tau) - \varphi(a)$  is equal to zero at the point  $\tau = a$ . Then, under  $\varepsilon \rightarrow 0$  the first integral on the right-hand side of (8) has the limit (see Reference 7)

$$\lim_{\varepsilon \rightarrow 0} \int_a^b \frac{\varphi(\tau) - \varphi(a)}{\tau - t_2} d\tau = \frac{1}{2\pi i} \int_a^b \frac{\varphi(\tau) - \varphi(a)}{\tau - a} d\tau \quad (9)$$

Taking into account that

$$\int_a^b \frac{d\tau}{\tau - t_2} = \ln \frac{b - t_2}{t_2 - a} = \ln \frac{b - t_2}{\exp(i\alpha_2)} - \ln \varepsilon$$

and from (8) and (9) the property P.4 follows.

## 2.2. The integral $I_b^1 = (1/2\pi i) \int_a^b \varphi(\tau) d\tau / (\tau - b)$

Enclose  $b$  with a circle of sufficiently small radius  $\delta$  to cross  $ab$  at the point  $t_1$  (Figure 2). Suppose again the function  $\varphi(\tau) \in H$  class on  $ab$ .

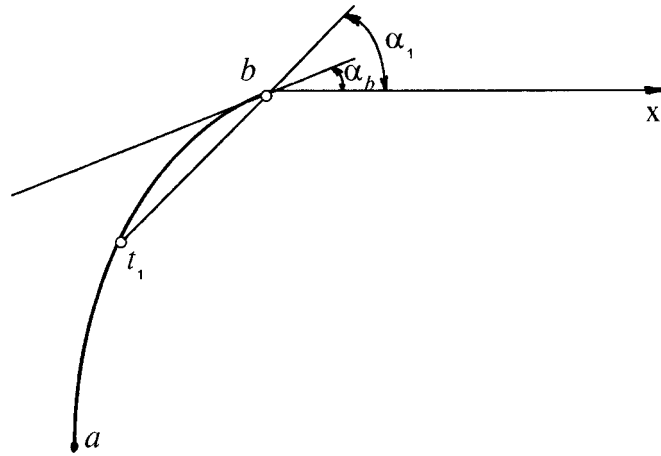


Figure 2. Geometry and co-ordinate system (singular point at the end of the arc)

Consider the *regular* integral

$$\frac{1}{2\pi i} \int_a^{t_1} \frac{\varphi(\tau) d\tau}{\tau - b} \quad (10)$$

It can be written in the form

$$\begin{aligned} \frac{1}{2\pi i} \int_a^{t_1} \frac{\varphi(\tau) d\tau}{\tau - b} &= \frac{1}{2\pi i} \int_a^{t_1} \frac{\varphi(\tau) - \varphi(b)}{\tau - b} d\tau + \frac{\varphi(b)}{2\pi i} \ln \frac{b - t_1}{b - a} \\ &= \frac{1}{2\pi i} \int_a^{t_1} \frac{\varphi(\tau) - \varphi(b)}{\tau - b} d\tau + \frac{\varphi(b)}{2\pi i} \ln \frac{\delta \exp(i\alpha_1)}{b - a} \end{aligned} \quad (11)$$

where the angle  $\alpha_1$  is shown in Figure 2.

Suppose by definition

$$\frac{1}{2\pi i} \int_a^b \frac{\varphi(\tau) d\tau}{\tau - b} \stackrel{\text{def}}{=} \lim_{\varepsilon \rightarrow 0} \left[ \frac{1}{2\pi i} \int_a^{t_1} \frac{\varphi(\tau) d\tau}{\tau - b} - \frac{\varphi(b)}{2\pi i} \ln \delta \right] \quad (12)$$

We get from (11) and (12)

$$\frac{1}{2\pi i} \int_a^b \frac{\varphi(\tau) d\tau}{\tau - b} = \frac{1}{2\pi i} \int_a^b \frac{\varphi(\tau) - \varphi(b)}{\tau - b} d\tau + \frac{\varphi(b)}{2\pi i} \ln \frac{\exp(i\alpha_b)}{b - a} \quad (13)$$

where the angle  $\alpha_b$  is shown in Figure 2.

The properties P.1–P.3 will be valid for the integral defined by (12) if one changes ‘ $a$ ’ for ‘ $b$ ’ in the corresponding formulae.

The property P.4 will take the form

$$\frac{1}{2\pi i} \int_a^b \frac{\varphi(\tau) d\tau}{\tau - b} = \lim_{\delta \rightarrow 0} \left[ \frac{1}{2\pi i} \int_a^b \frac{\varphi(\tau) d\tau}{\tau - t_1} - \frac{\varphi(b)}{2\pi i} \ln \delta \right]$$

Some new properties can now be proved

P.5.

(a)

$$\frac{1}{2\pi i} \int_a^b \frac{\varphi(\tau) d\tau}{\tau - a} = -\frac{1}{2\pi i} \int_b^a \frac{\varphi(\tau) d\tau}{\tau - a}$$

(b)

$$\frac{1}{2\pi i} \int_a^b \frac{\varphi(\tau) d\tau}{\tau - b} = -\frac{1}{2\pi i} \int_b^a \frac{\varphi(\tau) d\tau}{\tau - b}$$

P.6. If  $c \in ab$ , then

$$\frac{1}{2\pi i} \int_a^b \frac{\varphi(\tau) d\tau}{\tau - c} = \frac{1}{2\pi i} \int_a^c \frac{\varphi(\tau) d\tau}{\tau - c} + \frac{1}{2\pi i} \int_c^b \frac{\varphi(\tau) d\tau}{\tau - c}$$

where the integral on the left-hand side of the last equality is the CPV one.

To prove formula P.5(a), we consider the integral

$$-\frac{1}{2\pi i} \int_b^a \frac{\varphi(\tau) d\tau}{\tau - a}$$

By using the formulae (7) and (13), we get

$$\begin{aligned} -\frac{1}{2\pi i} \int_b^a \frac{\varphi(\tau) d\tau}{\tau - a} &= -\left\{ \frac{1}{2\pi i} \int_b^a \frac{\varphi(\tau) - \varphi(a)}{\tau - a} d\tau + \frac{\varphi(a)}{2\pi i} \ln \frac{\exp[i(\alpha_a + \pi)]}{a - b} \right\} \\ &= \frac{1}{2\pi i} \int_a^b \frac{\varphi(\tau) - \varphi(a)}{\tau - a} d\tau + \frac{\varphi(a)}{2\pi i} \ln \left\{ \frac{\exp[i(\alpha_a + \pi)]}{a - b} \right\}^{-1} \\ &= \frac{1}{2\pi i} \int_a^b \frac{\varphi(\tau) - \varphi(a)}{\tau - a} d\tau + \frac{\varphi(a)}{2\pi i} \ln \frac{b - a}{\exp(i\alpha_a)} = \frac{1}{2\pi i} \int_a^b \frac{\varphi(\tau)}{\tau - a} d\tau \end{aligned}$$

Property P.5(b) can be proved in the same way.

To prove P.6 we will use the definition of the CPV integral. From this definition and formulae (6) and (12), we get (suppose that  $\delta = \varepsilon$ )

$$\begin{aligned} \frac{1}{2\pi i} \int_a^b \frac{\varphi(\tau)}{\tau - c} d\tau &= \lim_{\varepsilon \rightarrow 0} \left[ \frac{1}{2\pi i} \int_a^{t_1} \frac{\varphi(\tau) d\tau}{\tau - c} + \frac{1}{2\pi i} \int_{t_2}^b \frac{\varphi(\tau) d\tau}{\tau - c} \right] \\ &= \lim_{\varepsilon \rightarrow 0} \left[ \frac{1}{2\pi i} \int_a^{t_1} \frac{\varphi(\tau) d\tau}{\tau - c} - \frac{\varphi(c)}{2\pi i} \ln \varepsilon + \frac{\varphi(c)}{2\pi i} \ln \varepsilon + \frac{1}{2\pi i} \int_{t_2}^b \frac{\varphi(\tau) d\tau}{\tau - c} \right] \\ &= \lim_{\varepsilon \rightarrow 0} \left[ \frac{1}{2\pi i} \int_a^{t_1} \frac{\varphi(\tau) d\tau}{\tau - c} - \frac{\varphi(c)}{2\pi i} \ln \varepsilon \right] + \lim_{\varepsilon \rightarrow 0} \left[ \frac{1}{2\pi i} \int_{t_2}^b \frac{\varphi(\tau) d\tau}{\tau - c} + \frac{\varphi(c)}{2\pi i} \ln \varepsilon \right] \\ &= \frac{1}{2\pi i} \int_a^c \frac{\varphi(\tau) d\tau}{\tau - c} + \frac{1}{2\pi i} \int_c^b \frac{\varphi(\tau) d\tau}{\tau - c} \end{aligned}$$

The same property will be valid if  $ab$  is a piecewise smooth curve and  $c$  is a corner point (Figure 3). The definition of CPV integral for this case was given by Muskhelishvili<sup>7</sup> (Appendix 2). This definition has the form

$$\frac{1}{2\pi i} \int_a^b \frac{\varphi(\tau) d\tau}{\tau - c} = - \left( 1 - \frac{\alpha}{2\pi} \right) \varphi(c) + \frac{\varphi(c)}{2\pi i} \ln \frac{b - c}{a - c} + \frac{1}{2\pi i} \int_a^b \frac{\varphi(\tau) - \varphi(c)}{\tau - c} d\tau$$

It can be rewritten as

$$\begin{aligned} \frac{1}{2\pi i} \int_a^b \frac{\varphi(\tau) d\tau}{\tau - c} &= \frac{\varphi(c)}{2\pi i} \ln \exp[i(\alpha - 2\pi)] + \frac{\varphi(c)}{2\pi i} \ln \frac{b - c}{a - c} + \frac{1}{2\pi i} \int_a^b \frac{\varphi(\tau) - \varphi(c)}{\tau - c} d\tau \\ &= \frac{1}{2\pi i} \int_a^b \frac{\varphi(\tau) - \varphi(c)}{\tau - c} d\tau + \frac{\varphi(c)}{2\pi i} \ln \left\{ \frac{b - c}{c - a} \exp[i\alpha - \pi] \right\} \end{aligned} \quad (14)$$

On the other hand, from (7) and (13), we have

$$\begin{aligned} \frac{1}{2\pi i} \int_a^c \frac{\varphi(\tau) d\tau}{\tau - c} + \frac{1}{2\pi i} \int_c^b \frac{\varphi(\tau) d\tau}{\tau - c} &= \frac{1}{2\pi i} \int_a^c \frac{\varphi(\tau) - \varphi(c)}{\tau - c} d\tau + \frac{\varphi(c)}{2\pi i} \ln \frac{\exp(i\alpha_{c1})}{c - a} \\ &\quad + \frac{1}{2\pi i} \int_a^b \frac{\varphi(\tau) - \varphi(c)}{\tau - c} d\tau + \frac{\varphi(c)}{2\pi i} \ln \frac{b - c}{\exp(i\alpha_{c2})} \\ &= \frac{1}{2\pi i} \int_a^b \frac{\varphi(\tau) - \varphi(c)}{\tau - c} d\tau + \frac{\varphi(c)}{2\pi i} \ln \left\{ \frac{b - c}{c - a} \exp[i(\alpha_{c1} - \alpha_{c2})] \right\} \end{aligned} \quad (15)$$

where the angles  $\alpha_{c1}$ ,  $\alpha_{c2}$  are shown in Figure 3.

Taking into account that  $\exp[i(\alpha - \pi)] = \exp[i(\alpha_{c1} - \alpha_{c2})]$  and formulae (14) and (15), we get the proof of P.6 for the case of a piecewise smooth curve.

*Remark 1.* The validity of P.6 for the case of piecewise smooth curve is a ‘touchstone’ for the definition of (6) and (12). We could have defined the integrals  $I_a^1$ ,  $I_b^1$  in somehow different way (for example, we could have added  $\varphi(a) \ln(\iota_2 - a)/2\pi i$  in (6)), but the property P.6 would not have been valid in this case.

*Remark 2.* From the property P.3 it follows that the definitions (6) and (15) will be valid in case of any piecewise smooth curve.

*Remark 3.* The approximation functions (which may be different for the different elements) need to coincide at the common points  $c_i$  of the neighbouring elements when one solves the CHSIE by BEM. Otherwise, they will not represent the limit values of the analytic inside domain function when the inner point tends to the points  $c_i$ .

*Remark 4.* As it is well known the *real* one-sided integrals are not independent of simple changes of variables. This fact can be illustrated by the following example. Consider the real integral

$$\int_0^2 \frac{dx}{x} \quad (16)$$

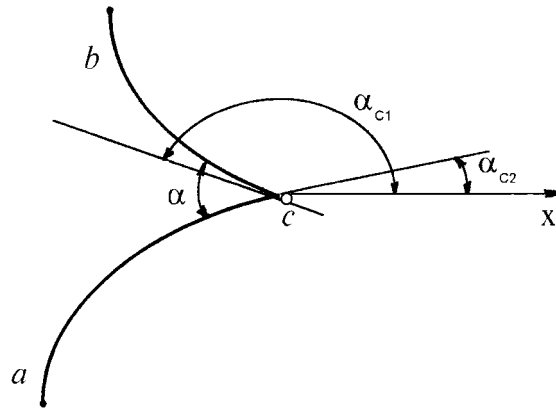


Figure 3. Geometry and co-ordinate system (singular point at the corner point of the arc)

According to the definition of real one-sided integral,<sup>22</sup> one has

$$\int_0^2 \frac{dx}{x} = \lim_{\varepsilon \rightarrow 0} \left( \int_0^2 \frac{dx}{x} + \ln \varepsilon \right) = \ln 2$$

But

$$\int_0^1 \frac{d(2t)}{2t} = \int_0^1 \frac{dt}{t} = \ln 1$$

Consider now the integral (16) as the complex one. We have from the formulae (6) and (7)

$$\int_0^2 \frac{dz}{z} = \ln \frac{2}{\exp(i\alpha_{z_0})} = \ln 2$$

because the angle  $\alpha_{z_0}$  between the point  $z_0 = 0 + 0i$  and axis  $x = \operatorname{Re}(z)$  is equal to zero (the integration is performed over the straight segment which links the beginning and end points of the integration curve). After the change of variables  $z = 2u$ , one has

$$\exp(i\alpha_{z_0}) = \frac{dz}{ds} = \frac{dz}{du} \frac{du}{ds} = 2 \frac{du}{ds}$$

where  $s$  is the arc's length. We have finally

$$\int_0^2 \frac{dz}{z} = \int_0^1 \frac{du}{u} = \ln \frac{1}{\partial u / \partial s} = \ln \frac{2}{\partial z / \partial s} = \ln \frac{2}{\exp(i\alpha_{z_0})} = \ln 2$$

and in that sense it is possible to change variables.

This example confirms again that the detailed analysis of the function properties is impossible without considering them in the complex plane.



### 3. HADAMARD'S INTEGRAL WITH THE SINGULAR POINT AT THE END POINT OF THE INTEGRATION CURVE

Suppose again that the integration curve is a smooth arc  $ab$  and assume that the function  $\varphi(\tau)$  has the derivative  $\varphi'(\tau) \in H$  class on  $ab$ .

3.1. The integral  $I_a^2 = (1/2\pi i) \int_a^b \varphi(\tau) d\tau / (\tau - a)^2$

Consider the *regular* integral

$$\frac{1}{2\pi i} \int_{t_2}^b \frac{\varphi(\tau) d\tau}{(\tau - a)^2} \quad (17)$$

where  $t_2$  is the point as shown in Figure 1.

It can be written as

$$\frac{1}{2\pi i} \int_{t_2}^b \frac{\varphi(\tau) - \varphi(a) - \varphi'(a)(\tau - a)}{(\tau - a)^2} d\tau + \frac{\varphi(a)}{2\pi i} \left[ \frac{1}{t_2 - a} - \frac{1}{b - a} \right] + \frac{\varphi'(a)}{2\pi i} \ln \frac{b - a}{t_2 - a}$$

Suppose by definition

$$I_a^2 = \lim_{\varepsilon \rightarrow 0} \left[ \frac{1}{2\pi i} \int_{t_2}^b \frac{\varphi(\tau) d\tau}{(\tau - a)^2} + \frac{\varphi'(a)}{2\pi i} \ln \varepsilon - \frac{\varphi(a)}{2\pi i} \frac{1}{t_2 - a} \right] \quad (18)$$

From these formulae it follows

$$\frac{1}{2\pi i} \int_a^b \frac{\varphi(\tau) d\tau}{(\tau - a)^2} = \frac{1}{2\pi i} \int_a^b \frac{\varphi(\tau) - \varphi(a) - \varphi'(a)(\tau - a)}{(\tau - a)^2} d\tau - \frac{\varphi(a)}{2\pi i} \frac{1}{b - a} + \frac{\varphi'(a)}{2\pi i} \ln \frac{b - a}{\exp(i\alpha_a)} \quad (19)$$

where the angle  $\alpha_a$  is shown in Figure 1 and the integral on the right-hand side of (19) is an improper one.

Taking into account that

$$\frac{1}{2\pi i} \ln \frac{b - a}{\exp(i\alpha_a)} = \frac{1}{2\pi i} \int_a^b \frac{d\tau}{\tau - a} \quad (20)$$

we have from (19), (20) and P.1

$$\frac{1}{2\pi i} \int_a^b \frac{\varphi(\tau) d\tau}{(\tau - a)^2} = \frac{1}{2\pi i} \int_a^b \frac{\varphi(a) - \varphi(a)}{(\tau - a)^2} d\tau - \frac{\varphi(a)}{2\pi i} \frac{1}{b - a} \quad (21)$$

where the integral on the right-hand side of (21) is a singular one (defined in Section 2.1).

The integral  $I_a^2$  defined by the formula (18) will satisfy the properties Q.1–Q.3 analogous to the properties P.1–P.3.

Q.1. If  $\varphi'_1(\tau), \varphi'_2(\tau) \in H$  class on  $ab$ , then

$$\frac{1}{2\pi i} \int_a^b \frac{\varphi_1(\tau) + \varphi_2(\tau)}{(\tau - a)^2} d\tau = \frac{1}{2\pi i} \int_a^b \frac{\varphi_1(\tau) d\tau}{(\tau - a)^2} + \frac{1}{2\pi i} \int_a^b \frac{\varphi_2(\tau) d\tau}{(\tau - a)^2}$$

Q.2. If  $k$  is any complex number, then

$$\frac{1}{2\pi i} \int_a^b k \frac{\varphi(\tau) d\tau}{(\tau - a)^2} = k \frac{1}{2\pi i} \int_a^b \frac{\varphi(\tau) d\tau}{(\tau - a)^2}$$

Q.3. If  $c \in ab$ , then

$$\frac{1}{2\pi i} \int_a^b \frac{\varphi(\tau) d\tau}{(\tau - a)^2} = \frac{1}{2\pi i} \int_a^c \frac{\varphi(\tau) d\tau}{(\tau - a)^2} + \frac{1}{2\pi i} \int_c^b \frac{\varphi(\tau) d\tau}{(\tau - a)^2}$$

The following new property is obtained:

Q.4.

$$\frac{1}{2\pi i} \int_a^b \frac{\varphi(\tau) d\tau}{(\tau - a)^2} = \frac{\varphi'(a)}{2\pi i} - \frac{\varphi(b)}{2\pi i} \frac{1}{b - a} + \frac{1}{2\pi i} \int_a^b \frac{\varphi'(\tau) d\tau}{\tau - a} \quad (22)$$

It can be proved easily by integrating the integral (17) by parts and taking into account (18) and (6). The formula (22) provides us the possibility to integrate the integral  $I_a^2$  by parts.

3.2. The integral  $I_b^2 = (1/2\pi i) \int_a^b \varphi(\tau) d\tau / (\tau - b)^2$

Similar to Section 3.1 we define this integral as ( $t_1$  and  $\delta$  are shown in Figure 2)

$$I_b^2 = \lim_{\delta \rightarrow 0} \left[ \frac{1}{2\pi i} \int_a^{t_1} \frac{\varphi(\tau) d\tau}{(\tau - b)^2} - \frac{\varphi'(b)}{2\pi i} \ln \delta + \frac{\varphi(b)}{2\pi i} \frac{1}{t_1 - b} \right] \quad (23)$$

and obtain the following formula to calculate it:

$$\frac{1}{2\pi i} \int_a^b \frac{\varphi(\tau) d\tau}{(\tau - b)^2} = \frac{1}{2\pi i} \int_a^b \frac{\varphi(\tau) - \varphi(b)}{(\tau - b)^2} d\tau - \frac{\varphi(b)}{2\pi i} \frac{1}{b - a} \quad (24)$$

where the integral on the right-hand side of (24) is a singular one (defined in Section 2.2).

The integral  $I_b^2$  will satisfy the properties Q.1–Q.3 if one changes ‘ $a$ ’ for ‘ $b$ ’ in the corresponding formulae.

The property Q.4 will have the form

$$\frac{1}{2\pi i} \int_a^b \frac{\varphi(\tau) d\tau}{(\tau - b)^2} = -\frac{\varphi'(b)}{2\pi i} - \frac{\varphi(a)}{2\pi i} \frac{1}{b - a} + \frac{1}{2\pi i} \int_a^b \frac{\varphi(\tau) d\tau}{\tau - b} \quad (25)$$

The following properties, analogous to P.5 and P.6 will be obtained:

Q.5.

(a)

$$\frac{1}{2\pi i} \int_a^b \frac{\varphi(\tau) d\tau}{(\tau - a)^2} = -\frac{1}{2\pi i} \int_b^a \frac{\varphi(\tau) d\tau}{(\tau - a)^2}$$

(b)

$$\frac{1}{2\pi i} \int_a^b \frac{\varphi(\tau) d\tau}{(\tau - b)^2} = -\frac{1}{2\pi i} \int_b^a \frac{\varphi(\tau) d\tau}{(\tau - b)^2}$$

Q.6. If  $c \in ab$ , then

$$\frac{1}{2\pi i} \int_a^b \frac{\varphi(\tau) d\tau}{(\tau - c)^2} = \frac{1}{2\pi i} \int_a^c \frac{\varphi(\tau) d\tau}{(\tau - c)^2} + \frac{1}{2\pi i} \int_c^b \frac{\varphi(\tau) d\tau}{(\tau - c)^2}$$

where the integral on the left-hand side of the last equality is a hypersingular one defined in References 16 and 17.

The proof of the properties Q.5(a) and (b) follows from formulae (21) and (24) and corresponding properties P.5(a) and (b).

The power Q.6 we will use the following definition of complex HFP integral (see References 16 and 17):

$$\frac{1}{2\pi i} \int_a^b \frac{\varphi(\tau) d\tau}{(\tau - c)^2} \stackrel{\text{def}}{=} \lim_{\varepsilon \rightarrow 0} \left[ \frac{1}{2\pi i} \int_a^{t_1} \frac{\varphi(\tau) d\tau}{(\tau - c)^2} + \frac{1}{2\pi i} \int_{t_2}^b \frac{\varphi(\tau) d\tau}{(\tau - c)^2} + \frac{\varphi(c)}{2\pi i} \left( \frac{1}{t_1 - c} - \frac{1}{t_2 - c} \right) \right]$$

From this definition and formulae (18) and (23) we have (suppose that  $\delta = \varepsilon$ )

$$\begin{aligned} \frac{1}{2\pi i} \int_a^b \frac{\varphi(\tau) d\tau}{(\tau - c)^2} &= \lim_{\varepsilon \rightarrow 0} \left[ \frac{1}{2\pi i} \int_a^{t_1} \frac{\varphi(\tau) d\tau}{(\tau - c)^2} + \frac{\varphi(c)}{2\pi i} \frac{1}{t_1 - c} - \frac{\varphi'(c)}{2\pi i} \ln \varepsilon \right] \\ &\quad + \lim_{\varepsilon \rightarrow 0} \left[ \frac{1}{2\pi i} \int_{t_2}^b \frac{\varphi(\tau) d\tau}{(\tau - c)^2} - \frac{\varphi(c)}{2\pi i} \frac{1}{t_2 - c} + \frac{\varphi'(c)}{2\pi i} \ln \varepsilon \right] \\ &= \frac{1}{2\pi i} \int_a^c \frac{\varphi(\tau) d\tau}{(\tau - c)^2} + \frac{1}{2\pi i} \int_c^b \frac{\varphi(\tau) d\tau}{(\tau - c)^2} \end{aligned}$$

The property Q.6 will be valid also in the case when  $ab$  is a piecewise smooth curve and  $c$  is a corner point. The definition of hypersingular integral for this case is given in References 16, 17 and 20.

The remarks analogous to the ones given at the end of Section 2 will be obtained. The only difference is in Remark 3. The approximation functions and *their derivatives* need to coincide at the common points of the neighbouring elements.

#### 4. APPLICATION TO BEM

Consider the applications to numerical solution by BEM of CHSIE for multiregions of interacting elastic bodies. This equation can be widely employed to a number of important geomechanical problems.

##### 4.1. CHSIE

This equation was obtained in Reference 17 by direct differentiating of the corresponding complex singular equation obtained by Linkov.<sup>9</sup> It can be written as

$$\begin{aligned} &\frac{1}{\pi i} \int_L \frac{\Delta u(\tau)}{(\tau - t)^2} d\tau + \frac{1}{2\pi i} \int_L \Delta u(\tau) S_1(\tau, t) d\tau - \frac{1}{2\pi i} \int_L \overline{\Delta u(\tau)} S_2(\tau, t) d\bar{\tau} \\ &\quad + \frac{1}{\pi i} \int_L \left( a_1 - \frac{a_3}{2} \right) \frac{\sigma(\tau)}{\tau - t} d\tau + \frac{1}{2\pi i} \int_L (a_1 - a_3) \sigma(\tau) S_3(\tau, t) d\tau \\ &\quad - \frac{1}{2\pi i} \int_L a_1 \overline{\sigma(\tau)} S_4(\tau, t) d\bar{\tau} - \frac{a_2}{2} \sigma(t) = f(t), \quad t \in L \end{aligned} \quad (26)$$

where  $L$  is the totality of external and internal boundaries;  $\Delta u = u^+ - u^-$  is the displacement discontinuity (DD);  $u^+$  and  $u^-$  are the limit values of the displacements if we approach the contour from its left or right side, respectively;  $\sigma = \sigma_n + i\sigma_\tau$ ;  $\sigma_n$  is a normal and  $\sigma_\tau$  is a shear traction on  $L$ ; the unit normal  $n$  is directed to the right of the direction of travel; the direction of travel is arbitrary for contact boundaries between regions; it is counterclockwise for the external boundary; a bar over a symbol denotes complex conjugation; the origin of the co-ordinate system is assumed to be inside some region;  $i = \sqrt{-1}$ ;

$$a_1 = \frac{1}{2\mu^+} - \frac{1}{2\mu^-}, \quad a_2 = \frac{1 + \kappa^+}{2\mu^+} + \frac{1 + \kappa^-}{2\mu^-}, \quad a_3 = \frac{1 + \kappa^+}{2\mu^+} - \frac{1 + \kappa^-}{2\mu^-}$$

$\kappa = 3 - 4\nu$  in plane strain,  $\kappa = (3 - \nu)/(1 + \nu)$  in plane stress,  $\mu^+$ ,  $\mu^-$  are the shear moduli of the contracting regions,  $\nu^+$ ,  $\nu^-$  are their Poisson's ratios, the sign '+' ('-') indicates the elastic constants for the region that is to the left (right) of the direction of travel on  $L$ :

$$f(t) = \frac{\kappa_\infty + 1}{4\mu_\infty} \left[ \sigma_{xx}^\infty + \sigma_{yy}^\infty + \frac{d\bar{t}}{dt} (\sigma_{xx}^\infty - \sigma_{yy}^\infty - 2i\sigma_{xy}^\infty) \right],$$

$\sigma_{xx}^\infty$ ,  $\sigma_{yy}^\infty$ ,  $\sigma_{xy}^\infty$  are the stresses at infinity (for a finite region these stresses are equal to zero);  $t = x + iy$ :

$$\begin{aligned} S_1(\tau, t) &= -\frac{\partial^2}{\partial \tau \partial t} \ln \frac{\tau - t}{\bar{\tau} - \bar{t}} = \frac{d\bar{t}}{dt} \frac{d\bar{\tau}}{d\tau} \frac{1}{(\bar{\tau} - \bar{t})^2} - \frac{1}{(\tau - t)^2} \\ S_2(\tau, t) &= \frac{\partial^2}{\partial \bar{\tau} \partial t} \ln \frac{\tau - t}{\bar{\tau} - \bar{t}} = \left( 1 + \frac{d\bar{t}}{dt} \frac{d\bar{\tau}}{d\tau} \right) \frac{1}{(\bar{\tau} - \bar{t})^2} - 2 \frac{d\bar{t}}{dt} \frac{\tau - t}{(\bar{\tau} - \bar{t})^3} \\ S_3(\tau, t) &= \frac{\partial}{\partial t} \ln \frac{\tau - t}{\bar{\tau} - \bar{t}} = \frac{d\bar{t}}{dt} \frac{1}{\bar{\tau} - \bar{t}} - \frac{1}{\tau - t} \\ S_4(\tau, t) &= -\frac{\partial}{\partial t} \ln \frac{\tau - t}{\bar{\tau} - \bar{t}} = \frac{1}{\bar{\tau} - \bar{t}} - \frac{d\bar{t}}{dt} \frac{\tau - t}{(\bar{\tau} - \bar{t})^2}. \end{aligned} \quad (27)$$

We take  $1/2\mu^- = 0$ ,  $u^- = 0$  for an external boundary of a finite system of regions;  $1/2\mu^+ = 0$ ,  $u^+ = 0$  for a plane with a hole.

To exclude rigid-body movement (if only tractions are given on the whole outer contour) the following additional conditions are introduced:

$$\int_L \frac{\Delta u(\tau)}{\tau - z_0} d\tau = 0 \quad \text{Re} \int_L \frac{\Delta u(\tau)}{(\tau - z_0)^2} d\tau = 0 \quad (28)$$

where the point  $z_0$  belongs to the interior region.

Boundary and contact conditions may be different on different parts of  $L$  and may include prescribed tractions, or DD, or prescribed relationships between tractions and DD.

Note that equation (26) accounts for cracks if one puts  $\mu^+ = \mu^- = \mu$ ;  $\kappa^+ = \kappa^- = \kappa$ , for corresponding parts of  $L$  (then  $a_1 = a_3 = 0$  for these parts).

#### 4.2. Numerical algorithm and numerical results

The universal algorithm to solve this equation was suggested in Reference 27. It is based on BEM. The basic idea is a possibility of the smooth approximation of each smooth part of the boundary by a number of circular arcs and straight elements. So, only two types of the boundary elements are employed. If unknown functions are approximated by the polynomials or the polynomials multiplied by a weight function (for the tip elements) all the integrals (hypersingular, singular and regular) involved in this equation can be evaluated in a closed form. The expressions to evaluate the integrals involved in (26) are given in Reference 27.

We will apply this method to the solution of two problems: a circular hole and a circular elastic inclusion in an infinite plate.

In case when the collocation points coincide with the end points of the boundary elements the formulae (7), (13), (21) and (24) will be used to evaluate the singular and hypersingular integrals involved in (26).

**4.2.1. An elastic circular inclusion in an infinite plate.** Suppose the DD are equal to zero at the boundary of the inclusion. In this case the CHSIE (26) can be considered as the CSIE with the traction  $\sigma = \sigma_n + i\sigma_\tau$  as the unknown function.

Consider the two types of the conditions at infinite shown in Figures 4(a) and (b).

Both of these problems have the analytical solutions<sup>6</sup>

$$(a) \quad \begin{cases} \sigma_n = \beta_0 \\ \sigma_\tau = 0 \end{cases}, \quad (b) \quad \begin{cases} \sigma_n = (\beta_0 + \delta_0 \cos 2\theta)/2 \\ \sigma_\tau = -(\delta_0 \sin 2\theta)/2 \end{cases}$$

where

$$\beta_0 = \frac{\mu_0(\kappa + 1)}{2\mu_0 + \mu(\kappa_0 - 1)}, \quad \delta_0 = \frac{\mu_0(\kappa + 1)}{\mu + \mu_0\kappa}$$

the angle  $\theta$  and the elastic constants are shown in Figure 4.

Suppose the elastic constants for both problems are equal to

$$\kappa_0 = \kappa = 1, 8, \quad \mu_0/\mu = 3$$

Then we have the following analytical solutions for the problems considered:

$$(a) \quad \begin{cases} \sigma_n = 1.2352941 \\ \sigma_\tau = 0 \end{cases} \quad (b) \quad \begin{cases} \sigma_n = 0.61764705 + 0.65625 \cos 2\theta \\ \sigma_\tau = -0.65625 \sin 2\theta \end{cases}$$

Both problems were solved by BEM. The circular arcs of the equal lengths were used as the boundary elements. The unknown function  $\sigma$  was approximated by Lagrange polynomials of the second degree. The nodes of the Lagrange polynomials at each element were placed as follows.

One of them was placed at the centre point of the element. The other two nodes were located in two different ways:

- (i) at the end points of the element,
- (ii) at the inner points of the element which divide it in the relation  $1/k$  and  $(k-1)/k$  respectively,  $k = 3, 4, \dots, 15$ .

The conventional collocation technique was used to solve CHSIE. The collocation points were chosen to coincide with the nodes of the Lagrange polynomials.

We will discuss the numerical results obtained for the problems (a) and (b).

(a) *The case of the uniform tension* (Figure 4(a)): In this case the quadric approximation provides an exact solution, whatever the number of boundary elements may be. For the boundary of the inclusion the number of the elements was varied from 3 to 24. The collocation points for each of these cases were placed in two ways as we agreed before. The results were the same for all schemes considered and depend weakly on the ways to place the collocation points. The normal traction at each collocation point was equal to 1.2352940. This value coincides with the analytical solution up to 7 digits. In the case when the collocation points were placed at the inner points of the element the value of the unknown function at the end points of the elements were calculated in two different ways (by using the Lagrange polynomials for each of the neighbouring elements). The values obtained coincided with each other and with the analytical solution up to 7 digits. It means that the continuity constraint was satisfied even in the case when the collocation points (and nodes) were away from the edge ones.

The use of the collocation points at the end points of the element decreases the number of nodes. But in our case it was not so important. Thus, if the number of the boundary element is equal to 3 (as we can see it provides an excellent precision), we have 7 nodes in the case (i) and 9 nodes in the case (ii).

(b) *The case of the uniaxial tension* (Figure 4(b)): In this case the quadratic approximation does not provide an exact solution. So, we can expect that the accuracy of the calculations will depend on the number of elements. It was really so for both cases of node locations.

To compare the results obtained by using the different ways of locating the nodes, consider that  $n = 12$  ( $n$  is the number of the boundary elements). The tractions ( $\sigma_n + i\sigma_\tau$ ) at the mid-points of the boundary elements for schemes (i) and (ii) are shown in Tables 1 and 2, respectively. Due to the symmetry only a part of the results are shown. The results for scheme (ii) of the nodes situation were quite sensitive to the value of  $k$ . The best results were in the case when  $k = 4$  and they became worse when  $k$  increases. But for all values of  $k$  they were correct up to 3 digits. The best case ( $k = 4$ ) provides the results which were correct up to 4 digits.

We can see from Tables I and II that the results in case (ii) are better than in case (i). But in case (i) the number of nodes is equal to  $m = 2n + 1 = 25$  and is less than in case (ii) ( $m = 3n = 36$ ). The consideration of the cases when the number of nodes is the same but the number of the elements is different leads to analogous results. We can conclude that the situation of the collocation points at the end points of the elements does not lead to the sufficient improvement of accuracy if the polynomial approximation of the unknown functions is used. The more important factor is the 'quality' of the approximations.

To show it we take into account that the analytical solution of the problem (b) can be written as

$$\sigma = \sigma_n + i\sigma_\tau = 0.61764705 + 0.65625\bar{\tau}^2$$

We will now use the following approximation for  $\sigma$ :

$$\sigma = a_0 + a_1\bar{\tau} + a_2\bar{\tau}^2$$

It corresponds to the representation of the function  $\sigma\tau^2$  by the Lagrange polynomial of the second order and allows us to use the numerical algorithm suggested in Reference 27. For the boundary

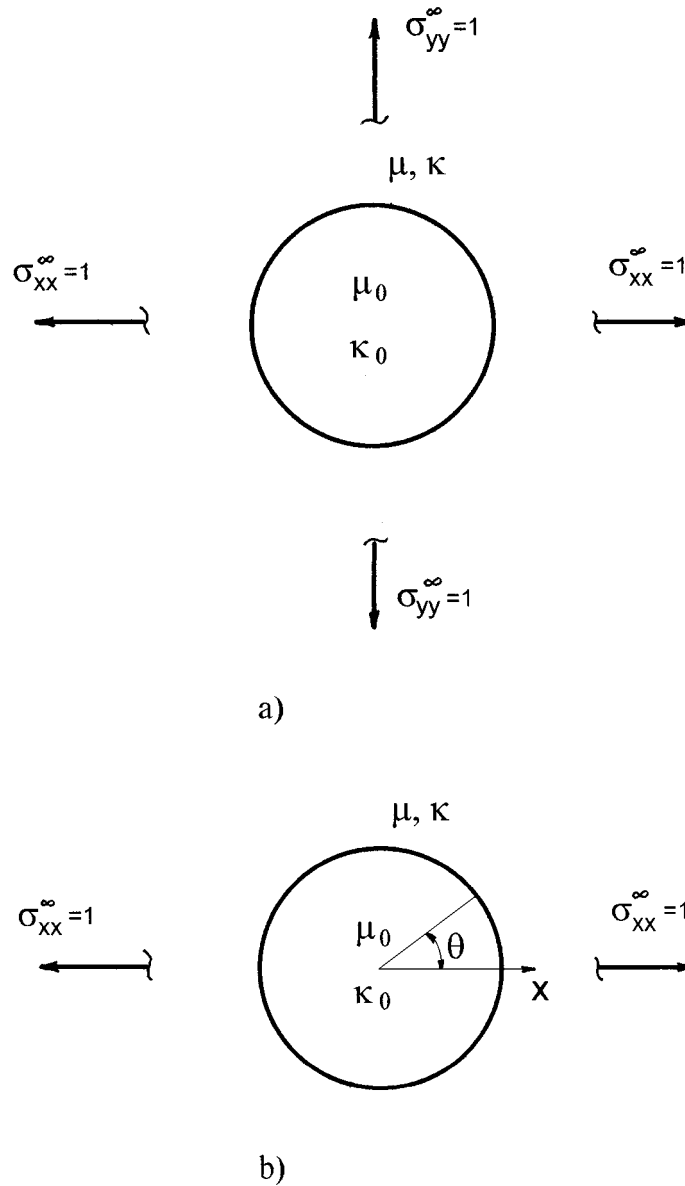


Figure 4. Geometry and loading for the circular elastic inclusion: (a) uniform tension: (b) uniaxial tension

of the inclusion the number of the elements was varied again from 3 to 24 and collocation points for each of these cases were placed in two ways as we agreed before. The results were the same for all the schemes considered and do not depend on the ways to place the collocation points. They coincide with the analytical solution up to 7 digits.

Table I. The tractions at the mid-points of the elements (circular inclusion,  $n = 12$ )

$\theta$ (deg)	Analytic solution	Case (i)
15	$1.185976 - 0.328125i$	$1.188420 - 0.329533i$
45	$0.617647 - 0.656250i$	$0.617647 - 0.659067i$
75	$0.049318 - 0.328125i$	$0.046879 - 0.329533i$

Table II. The tractions at the mid-points of the elements (circular inclusion,  $n = 12$ )

$\theta$ (deg)	Case (ii), $k = 4$	Case (ii), $k = 5$	Case (ii), $k = 13$
15	$1.185836 - 0.328045i$	$1.186204 - 0.328258i$	$1.18740 - 0.328946i$
45	$0.617646 - 0.656089i$	$0.617647 - 0.656515i$	$0.617647 - 0.657891i$
75	$0.049457 - 0.328045i$	$0.049089 - 0.328258i$	$0.047898 - 0.328946i$

4.2.2. *The hole at the infinite plate.* Consider the problems shown in Figures 5(a) and (b). The tractions are equal to zero at the boundary of the hole, and from (26) the CHSIE with the DD as the unknown function need be considered.

Both problems have the analytical solutions (see Reference 6). Suppose, for simplicity  $\mu = 0.5$ ,  $\nu = 0.0$ .

The analytical solutions take the form

$$(a) \quad \Delta u_x + i\Delta u_y = 2\tau, \quad (b) \quad \begin{cases} \Delta u_x = 3 \cos \theta \\ \Delta u_y = -\sin \theta \end{cases}$$

To solve the problems by BEM we again represent the boundary of the hole by the circular arcs of equal lengths and approximate the DD by Lagrange polynomials of the second degree. The nodes of the polynomials will be placed, as we agreed, in the first example. The collocation points will coincide with the nodes of the polynomials.

(a) *The case of the uniform tension* (Figure 5(a)): In this case the quadratic approximation provides an exact solution, whatever the number of boundary elements may be. To compare the results obtained, consider the schemes with the same number of nodes ( $m = 9$ ). The number of the elements will be unequal:  $n = 4$  for case (i) and  $n = 3$  for case (ii). The results in both schemes have approximately the same precision and depend weakly on the ways to place collocation points. They coincide with the exact solutions up to 6 digits. In case (ii) the values of the unknown function and its derivative were calculated at the common points of the neighbouring elements by using two different Lagrange polynomials on each of the elements. They coincided with each other and with the analytical solution up to 6 digits. So, the continuity constraint was satisfied automatically.

(b) *The case of uniaxial tension* (Figure 5(b)): In this case the quadratic approximation does not provide an exact solution. The results ( $\Delta u = \Delta u_x + i\Delta u_y$ ) for the schemes with the same number of the nodes ( $m = 33$ ) are shown in Tables III and IV. The results are shown only for the first quadrant. The nodes for these two cases are different. For scheme (ii) of the situation of the



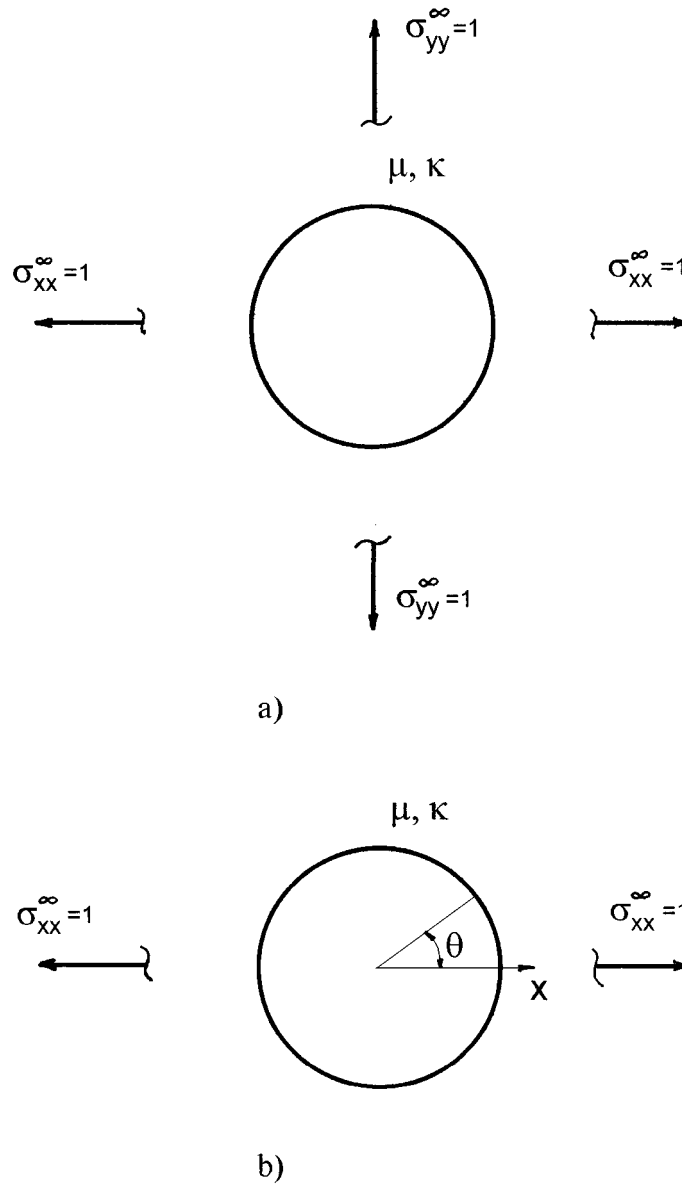


Figure 5. Geometry and loading for the hole: (a) uniform tension: (b) uniaxial tension

nodes the results (as in the second example from Section 4.2.1) were sensitive to the value of  $k$ . The best results ( $k = 13$ ) are shown in Table IV.

We can see that the accuracy of the results in case (ii) is much better in comparison with case (i). It is so, because the continuity constraint is not satisfied in case (i) (the left and right derivatives at the collocation points were not equal to each other). In both schemes of node locations the

Table III. DD at the nodes (hole, case (i))

$\theta$ (deg)	Analytical solution	Numerical solution
0·0	3·00000 + 0·00000 <i>i</i>	2·91180 – 0·00009 <i>i</i>
11·25	2·94236 – 0·19509 <i>i</i>	2·87133 – 0·18103 <i>i</i>
22·5	2·77164 – 0·38268 <i>i</i>	2·68999 – 0·34894 <i>i</i>
33·75	2·49441 – 0·55557 <i>i</i>	2·43416 – 0·51533 <i>i</i>
45·0	2·12132 – 0·70711 <i>i</i>	2·05886 – 0·64460 <i>i</i>
56·25	1·66671 – 0·83147 <i>i</i>	1·62653 – 0·77118 <i>i</i>
67·5	1·14805 – 0·92388 <i>i</i>	1·11437 – 0·84219 <i>i</i>
78·75	0·58527 – 0·98079 <i>i</i>	0·57130 – 0·90965 <i>i</i>
90·0	0·00000 – 1·00000 <i>i</i>	0·00019 – 0·91158 <i>i</i>

Table IV. DD at the nodes (hole, case (ii))

$\theta$ (deg)	Analytical solution	Numerical solution
2·517	2·99710 – 0·04392 <i>i</i>	2·99710 – 0·04487 <i>i</i>
16·364	2·87848 – 0·28173 <i>i</i>	2·87711 – 0·28114 <i>i</i>
30·210	2·59257 – 0·50317 <i>i</i>	2·59309 – 0·50199 <i>i</i>
35·245	2·45008 – 0·57707 <i>i</i>	2·44925 – 0·57798 <i>i</i>
49·091	1·96458 – 0·75575 <i>i</i>	1·96346 – 0·75468 <i>i</i>
62·937	1·36491 – 0·89051 <i>i</i>	1·36572 – 0·89001 <i>i</i>
67·972	1·12518 – 0·9270 <i>i</i>	1·12374 – 0·92754 <i>i</i>
81·818	0·42695 – 0·98982 <i>i</i>	0·42637 – 0·98858 <i>i</i>

accuracy increases when the number of the elements increases. But the character of the results was the same. Scheme (ii) provides better results in comparison with case (i). If we will again use the proper approximation for  $\Delta u$

$$\Delta u = a_0 + a_1 \bar{\tau} + a_2 \tau$$

taking into account that the analytical solution of this problem has a form  $\Delta u = 2\bar{\tau} + \tau$ ) we again get excellent results for all of the schemes of collocation points. They coincide with the analytical solution up to 6 digits.

## 5. APPLICATION TO GEOMECHANICAL PROBLEMS

As it was mentioned above, equation (26) can be widely employed to a number of important geomechanical problems. These problems usually have a large scale and the appropriate choice of the approximating functions can reduce computational costs dramatically.

Consider here as an example the problem of a rock with the circular opening near the fault (in a form of a fracture). The geometry of the problem is shown in the Figure 6. Suppose that the rock can be considered as an isotropic media with the following elastic constants and initial stresses (we suppose here that the sign ‘–’ corresponds to the case of tensile stresses)

$$\sigma_{yy} = -5000k \text{ Pa}, \quad -\sigma_{yy}/E = 10^{-3}, \quad \sigma_{xx}/\sigma_{yy} = 0.5, \quad \sigma_{xy} = 0, \quad \nu = 0.2$$

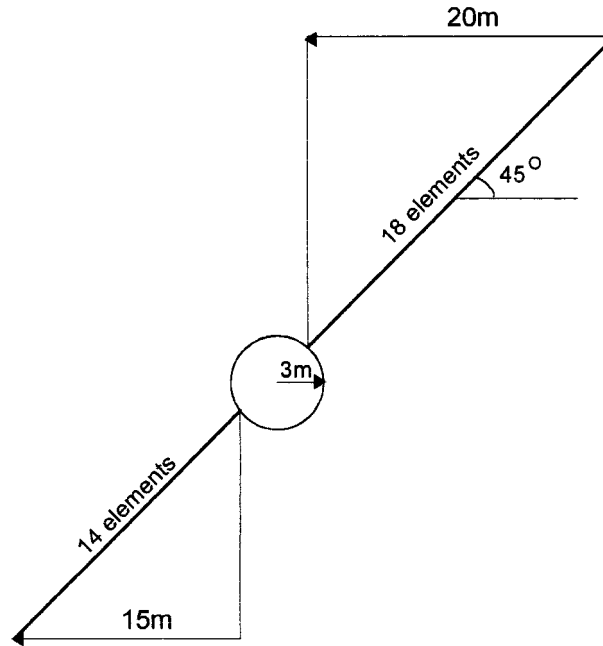


Figure 6. Geometry of the circular opening in the vicinity of the fracture

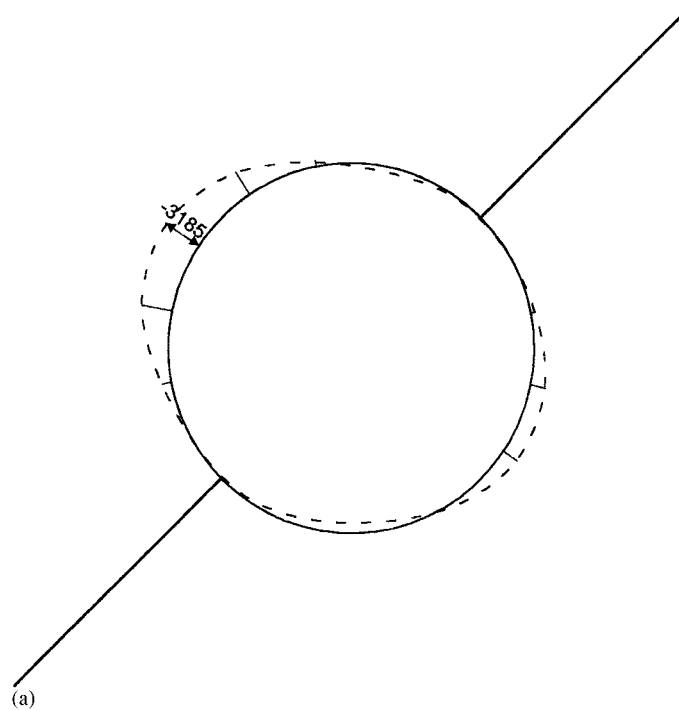


Figure 7. The stress component  $\sigma_{00}$  on the boundary of the opening: (a) traction-free boundary of the fracture; (b) the conditions  $\sigma_n = -K_n \Delta u_n$ ,  $\sigma_\tau = -K_\tau \Delta u_\tau$  are given at the fracture's boundary; (c) the opening without fracture

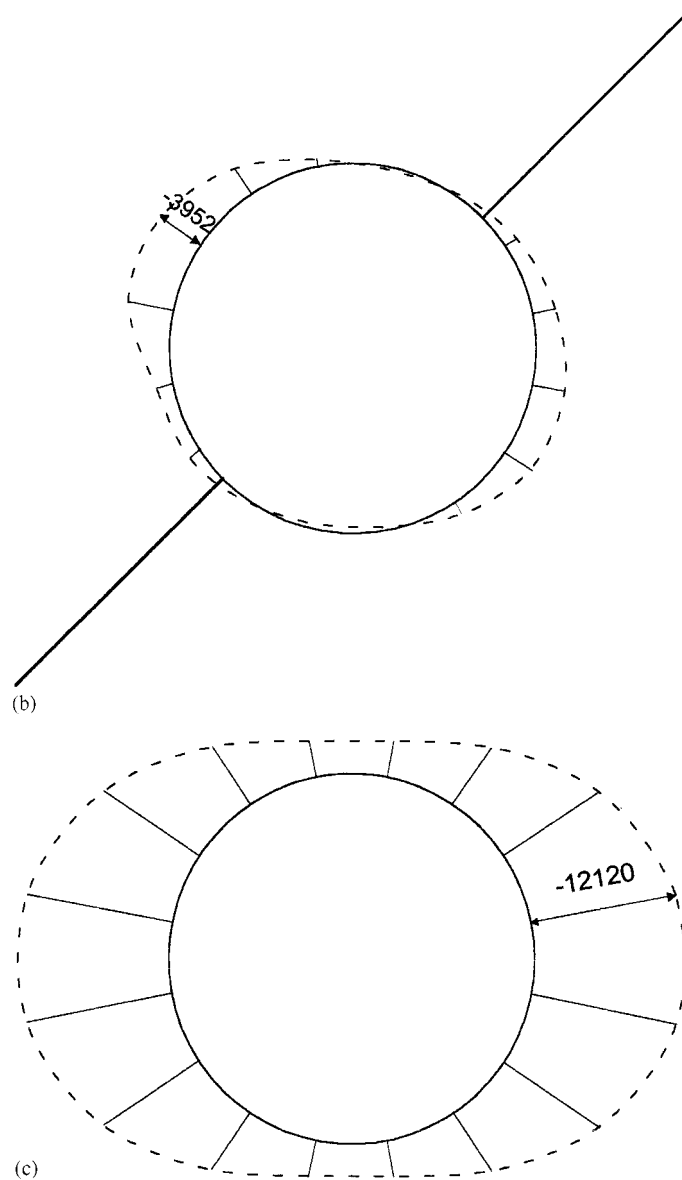


Figure 7. (continued)

The traction-free boundary of the opening is approximated by 16 circular conforming elements. The fracture was approximated by 32 straight elements as it is shown in Figure 6. Two cases of the boundary conditions on the fracture surface are considered:

- (i) tractions free surface;
- (ii) the conditions  $\sigma_n = -K_n \Delta u_n$ ,  $\sigma_\tau = -K_\tau \Delta u_\tau$  given at the boundary (we suppose that  $K_n = K_\tau = 10^4$  kPa/m).

The results (stress component  $\sigma_{\theta\theta}$  on the boundary of the opening) for both cases are shown in the Figures 7(a) and (b) and compared with the ones for the circular opening without crack (Figure 7(c)). The value of the stress  $\sigma_{\theta\theta}$  at each point corresponds to the length of the straight segment which links this point with the centre of the circle. We can see that the presence of the fracture breaks the symmetry and leads to the decrease in the stress  $\sigma_{\theta\theta}$ . At the same time the small zone of tensile stresses appear at the roof and floor of the opening.

## 6. CONCLUSIONS

Complex one-sided integrals of Cauchy and Hadamard can serve a useful means to solve CSIEs and CHSIEs by BEM. They allow us to place the collocation points and calculate the unknown elastic components at any points of the boundary (all the boundary points have now 'the equal rights'). It was shown that the use of conforming elements (when the collocation points coincide with the end points of the elements) does not improve accuracy dramatically. The 'quality' of the approximations is more important than the location of nodes. If the approximation provides the exact solution the continuity constraint is satisfied automatically. So, the only way to improve accuracy is to use better approximations. The first step in this direction is to consider the polynomials with complex conjugate terms. The new technique can be successfully used for numerical solutions to geomechanical problems by BEM.

## REFERENCES

1. P. Van Der Veer, 'Calculation methods for two-dimensional groundwater flow', Ph.D. Thesis. Delft Univ. of Technology, Netherlands, 1978.
2. B. Hunt and L. Isaacs, 'Integral equation formulation for groundwater flow', *J. Hyd. Div. ASCE*, **107**(HY10), 1197–1209 (1981).
3. T. Hromadka, II and C. Lai, *The Complex Variable Boundary Element Method in Engineering Analysis*, Springer, New York, 1987.
4. O. Strack, *Groundwater Mechanics*, Prentice-Hall, Englewood Cliffs, NJ, 1989.
5. C. Detournay and O. Strack, 'A new approximate technique for the hodograph method in groundwater flow and its application to coastal aquifers', *Water Resour. Res.*, **24**(9), 1471–1481 (1988).
6. N. I. Muskhelishvili, *Some Basic Problems of the Mathematical Theory of Elasticity*, Noordhoff, Netherlands, 1977.
7. N. I. Muskhelishvili, *Singular Integral Equations*, Noordhoff, Netherlands, 1977.
8. A. Linkov, 'Integral equations of the theory of elasticity for a plane with cuts loaded with equilibrated system of forces', *Dokl. Akad. Nauk SSSR*, **218**(6), 1294–1297 (1974) (in Russian).
9. A. Linkov, 'Plane problems of the static loading of a piecewise homogeneous linearly elastic medium', *J. Appl. Math. Mech.*, **47**, 527–532 (1983).
10. M. Savruk, *Two-Dimensional Problems of Elasticity for Body with Crack*, Naukova Dumka, Kiev, 1981 (in Russian).
11. V. Parton and P. Perlin, *Integral Equations in Elasticity*, Mir, Moscow, 1982.
12. P. S. Theocaris and N. I. Ioakimidis, 'On the solution of the problem of a curvilinear crack in a finite plane elastic medium', *Int. J. Fract.*, **15**(1), R7–R10 (1979).
13. P. S. Theocaris and G. J. Tsamasphyros, 'On the solution of boundary-value problems in plane elasticity for multiple-connected regions. I. The second boundary value problem', *Lett. Appl. Engng. Sci.*, **3**(3), 167–176 (1975).
14. Y. Z. Chen and N. Hasebe, 'Interaction of two curved cracks in an infinite plate', *Arch. Appl. Mech.*, **62**, 147–157 (1992).
15. A. Linkov and S. Mogilevskaya, 'Hypersingular integrals in plane problems of the theory of elasticity', *J. Appl. Math. Mech.*, **54**, 93–99 (1990).
16. A. Linkov and S. Mogilevskaya, 'Complex hypersingular integrals and integral equations in plane problems of elasticity theory', in *Researches on Structure Mechanics and Materials*, Leningrad Inst. for Build. Engng., Leningrad, 1991, pp. 17–34 (in Russian).
17. A. Linkov and S. Mogilevskaya, 'Complex hypersingular integrals and integral equations in plane elasticity', *Acta Mech.*, **105**, 189–205 (1994).

18. A. Linkov, V. Zubkov and S. Mogilevskaya, 'Complex integral equations: an effective means to solve plane problems', *Preprint No. 118*, Institute for Problems of Mech. Engng. (Russian Academy of Science) 1994, (in Russian).
19. A. Linkov and S. Mogilevskaya, 'On the theory of complex hypersingular equations', in S. Atluri, G. Yagawa and T. Cruse (eds), *Computational Mech.*'95, Vol. 2, Berlin, 1995, pp. 2836–2840.
20. E. Ladopoulos, 'New aspects for the generalization of the Sokhotski–Plemelj formulae for the solution of finite-part singular integrals used in fracture mechanics', *Int. J. Fract.* **54**, 317–328 (1992).
21. L. Chikin, Riemann's boundary-value problem's and singular integral equation's peculiar cases, *Uchen. Zapiski Kazansk. Univ.* **113**, 57–105 (1953) (in Russian).
22. J. Hadamard, *Lectures on Cauchy's Problem in Linear Partial Differential Equations*, Yale, University Press, Yale, 1923.
23. H. R. Kutt, 'The numerical evaluation of principal value integrals by finite part integration', *Numer. Math.*, **24**, 205–210 (1975).
24. C. Brebbia, J. Telles and L. Wrobel, *Boundary Element Techniques. Theory and Applications in Engineering*, New York, Springer, 1984.
25. P. A. Martin and F. J. Rizzo, Hypersingular integrals: how smooth must the density be? *Int. J. Numer. Meth. Engng.*, **39**, 687–704 (1996).
26. Q. Huang and T. A. Cruse, 'On the non-singular traction-BIE in elasticity', *Int. J. Numer. Meth. Engng.*, **37**, 2041–2072 (1999).
27. S. Mogilevskaya, 'The universal algorithm based on complex hypersingular integral equation to solve plane elasticity problems', *Comput. Mech.*, **18**, 127–138 (1996).